Journal of Physics: Conference Series **485** (2014) 012030 doi:10.1088/1742-6596/485/1/012030

A search for dark matter appearing as missing transverse energy at CMS

Tia Miceli for the CMS Collaboration

UC Davis Physics Department, 1 Shields Avenue, Davis, CA, 95616, USA

E-mail: miceli@physics.ucdavis.edu

Abstract. Results are presented of a search for dark matter production using the CMS detector at the LHC. Collisions of pp at $\sqrt{7}$ TeV totaling 5 fb^{-1} were counted for final states consisting of missing transverse energy accompanied by either a monophoton or a monojet. The data is consistent with Standard Model background, so limits are placed on both spin-dependent and spin-independent dark matter particle masses and production cross-sections. These are examined within the context of direct detection experiments where our results extend the current best limits.

1. Introduction

Proton-proton collisions from the Large Hadron Collider (LHC) totaling 5 fb^{-1} at $\sqrt{s} = 7$ TeV in which the final state contains a photon (γ) and missing transverse energy ($\not{E}_T$) or a jet and $\not{E}_T$ are used to investigate possible dark matter (DM) production. Dark matter is the dominant non-baryonic component of the universe's matter density [1]. Many searches for the DM particle (χ) rely on direct detection via a χ recoiling from a nucleus ($q\chi \rightarrow q\chi$), or DM annihilation observable in cosmic rays ($\chi\bar{\chi} \rightarrow \gamma\gamma$). At colliders however, this diagram is rotated and we look for $q\bar{q} \rightarrow \chi\bar{\chi}$. Since DM travels through the Compact Muon Solenoid detector [2] (CMS) without interaction, it appears as $\not{E}_T$ in the resulting collision fragments. To make this process visible, a γ or jet must be radiated from one of the incoming quarks. We study the monophoton and monojet final states.

Assuming a massive mediator couples with the incoming quarks and outgoing Dirac $\chi\bar{\chi}$ particles, the process can be contracted into an effective theory [3],[4]. The scale of the theory, Λ, is given by $\Lambda = M_m/\sqrt{g_\chi g_q}$, where M_m is the mediator mass, g_χ is its coupling to DM, and g_q is its coupling to quarks. This model provides a means to compare the t-channel χ-nucleon elastic scattering cross section to the s-channel DM pair production cross section. The effective operator could be either a vector operator leading to a spin-independent interaction, or an axial-vector operator leading to a spin-dependent interaction.

2. Monophoton

The monophoton data is selected from events that pass a single-photon trigger that is fully efficient within the signal region of $|\eta^\gamma| < 1.44$ (highest photon purity) and $p_T^\gamma > 145$ GeV.

The photon is identified as such by requiring the following isolation criteria. The p_T in the hadronic calorimeter (HCAL) within an annulus of $0.15 < \Delta R < 0.4$, where $\Delta R = \sqrt{(\Delta\eta)^2 + (\Delta\phi)^2}$, must be less than 2.2 GeV $+0.0025 \cdot p_T^\gamma$. The p_T in the electromagnetic

calorimeter (ECAL) within an annulus of $0.06 < \Delta R < 0.4$ but excluding deposits within $|\Delta\eta < 0.04|$ is less than 4.2 GeV $+0.006 \cdot p_T^{\gamma}$. The fraction of energy in the HCAL to the energy in the ECAL within the solid cone of $\Delta R < 0.4$ must be less than 0.05. The p_T of track originating from the photon's assigned vertex within an annulus of $0.04 < \Delta R < 0.4$ but excluding deposits within $|\Delta\eta| < 0.015$ must be less than 2.0 GeV $+0.001 \cdot p_T^{\gamma}$. It is also required that there are no tracker hits indicative of an electron (called a pixel seed). These ignored regions in $|\Delta\eta|$ ensure high photon identification efficiency for those photons that begin to shower within the tracker. Due to the high luminosity at the LHC, there may be multiple collisions at once, which may result in an ambiguity in the assignment of a photon's origin collision vertex. To account for this, the photon is also required to pass the track isolation criteria for all reconstructed vertices, and a systematic uncertainty is included.

The $\not{E}_T$ is the magnitude of the vector sum of all reconstructed particles in the event using the particle flow algorithm [5]. The $\not{E}_T$ requirement is optimized to be greater than 130 GeV to optimize the signal strength.

Events with excessive hadronic activity are removed by requiring that there are no particle flow jets, identified with the anti-k_T algorithm with a distance parameter of 0.5 [6], within $|\eta| < 3.0$ outside of $\Delta R(jet, \gamma) = 0.5$ and $p_T > 40$ GeV and that there are no tracks outside of $\Delta R(track, \gamma) = 0.04$ with $p_T > 20$ GeV.

Backgrounds unrelated to pp collisions are removed by further cuts. Protons that stray from the beam, can shower to muons that bremsstrahlung in the ECAL. These and showers from cosmic muons are reduced by vetoing muon tracks and requiring that the time assigned to the photon is ± 3 ns of that expected of a collision particle's arrival at the ECAL. Other anomalous ECAL signals are reduced by requiring that the timing of all the deposits comprising the photon are consistent [7].

Any backgrounds unrelated to pp collisions remaining are estimated from data by examining the transverse distribution of energy in the EM cluster and the time of arrival of the signal in the channel with the largest energy deposition. Templates for anomalous signals, cosmic-ray muons, and beam halo events are fitted to a candidate sample that has no timing requirement. It is found that only the halo muons give a significant residual contribution to the in-time sample with an estimated 11.1 ± 5.6 events.

Events of $W \to e\nu$ can mimic the monophoton signal, if the electron is misreconstructed. Estimating with MC simulated events and verifying with $Z \to ee$ events in data shows that the matching of electron showers to pixel seeds has an efficiency of $\epsilon = 0.9940 \pm 0.0025$. The contribution of $W \to e\nu$ events in the candidate sample is found by scaling a control sample of electron candidates by $(1 - \epsilon)/\epsilon$ yielding 3.5 ± 1.5 events.

The contamination from jets misidentified as photons is estimated by using a control sample of EM-enriched QCD events to calculate the ratio of events that pass the signal photon criteria relative to those that pass looser photon criteria but fail an isolation requirement. Since the EM-enriched sample also includes the production of direct single photons, this additional contribution to the ratio is estimated by fitting templates of energy-weighted shower widths from MC-simulated $\gamma + jets$ events to an independent QCD data sample. This contribution of true photons is subtracted from the numerator of the ratio. This corrected ratio is applied to a subset of the EM-enriched jet events that passes loose photon identification and additional monophoton event selection criteria, providing a background contribution of 11.2 ± 2.8 jet events.

The irreducible background, $Z(\to \nu\bar{\nu}) + \gamma$, as well as the $\gamma + jet$, $W(\to \ell\nu) + \gamma$, and diphoton backgrounds are estimated using Monte Carlo simulation.

A summary of the Standard Model (SM) backgrounds and the number of observed candidates are given in Table 1. Observation is consistent with the SM prediction.

Table 1. Monophoton backgrounds and observed events.

Process	Events
$Z(\nu\bar{\nu}) + \gamma$	45.3 ± 6.9
Non-collision BG	11.1 ± 5.6
$W \to e\nu$	3.5 ± 1.5
$jets$	11.2 ± 2.8
Other	4.1 ± 1.0
Total SM	75.1 ± 9.5
Data	73

3. Monojet

The monojet data is collected by jet triggers that are fully efficient within the candidate criteria that the highest p_T jet (j_1) is within $|\eta(j_1)| < 2.4$ with $p_T(j_1) > 110$ GeV.

The jet is reconstructed the same as the jets in previous section. A second jet, j_2 is allowed if $|\Delta\phi(j_1, j_2)| < 2.5$ radians to allow for accompanying initial or final state radiation while still rejecting dijet events. Furthermore, if there are additional jets with $p_T > 30$ GeV, the event is vetoed. To reduce events from W, Z, and top decays, events with isolated muons or electrons of $p_T > 10$ GeV are discarded. To be considered isolated, the lepton must be farther away from j_1 than $\Delta R = 0.3$ and the sum of the p_T of photons and hadronic particles within a cone of $\Delta R = 0.4$ divided by the lepton p_T is less than 0.2. Tau lepton decays are removed by vetoing events with isolated tracks of $p_T > 10$ GeV. An isolated track is one that requires that the sum of all tracks of $p_T > 1$ GeV within the annulus $0.02 < \Delta R < 0.3$ is less than 10% of the p_T of the track under consideration. Any instrumental backgrounds in the calorimeters are removed by requirements on neighboring channels or timing requirements.

The $\not\!\!E_T$ definition is the same as the previous except that muons are excluded from the calculation. Missing transverse energy value is optimized in MC to be greater than 350 GeV.

Background due to $Z(\to \nu\bar{\nu}) + jet$ is estimated from a control sample of $Z(\to \mu\bar{\mu}) + jet$ and scaled by the branching ratios, and is found to be 900 ± 94 events.

Background due to $W(\to \mu\nu)+jets$ is estimated by scaling a control sample of $W(\to \mu\nu)+jets$ by the muon reconstruction inefficiency. The background due to lost electrons and taus also use this control sample, but with a scaling produced by MC to determine the number of $W(\to e\nu) + jets$ and $W(\to \tau\nu) + jets$ and the appropriate reconstruction inefficiencies. The total $W + jets$ background is 312 ± 35 events.

The remaining backgrounds from QCD multijet events, $t\bar{t}$, and $Z(\ell\ell) + jets$ are small and are estimated from MC. The summary of monojet backgrounds and observed candidates are in Table 2. Observation agrees with the SM prediction.

4. Results

Upper limits are placed on the DM production cross sections, as a function of M_χ, assuming vector and axial-vector operators, summarized in Table 3 and Table 4. These are converted into the corresponding lower limits on the cutoff scale, Λ, also listed in Table 3 and Table 4. The Λ values are then translated into upper limits on the χ-nucleon cross sections, calculated within the effective theory framework. These are displayed in Fig. 1 and Fig. 2 as a function of M_χ. Also shown are the results from $p\bar{p}$ collider experiment CDF [8], direct detection experiments, COUPP [9], CoGeNT [10], Picasso [11], XENON100 [12], CDMS II [13, 14], and SIMPLE [15], and indirect detection experiments, IceCube [16] and Super-K [17]. Table 6 shows the 90%

Table 2. Monojet backgrounds and observed events.

Process	Events
$Z(\nu\bar{\nu}) + jets$	900 ± 94
$W + jets$	312 ± 35
$t\bar{t}$	8.5 ± 8.5
$Z(\ell\ell) + jets$	2.0 ± 2.0
Single t	1.1 ± 1.1
QCD Multijets	1.3 ± 1.3
Total SM	1225 ± 101
Data	1142

C.L. limits on Λ and the χ-nucleon cross section for the spin-dependent and spin-independent interactions.

Previously inaccessible χ masses below ~ 3.5 GeV are excluded for a χ-nucleon cross section greater than ~ 3 fb at 90% C.L. For spin-dependent scattering, the upper limits surpass all previous constraints for the mass range of 1-100 GeV. The results presented are valid for mediator masses larger than the limits on Λ, assuming unity for the couplings g_χ and g_q. The assumptions on χ interactions made in calculating the limits vary with experiments. Further, in the case of direct and indirect searches, an astrophysical model must be assumed for the density and velocity distribution of DM.

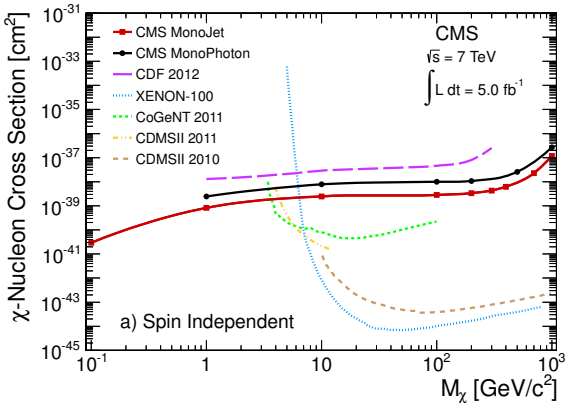

Figure 1. Comparison of the 90% CL upper limits on the dark matter-nucleon scattering cross section versus dark matter mass for the spin-independent (vector coupling) models with results from various direct detection experiments

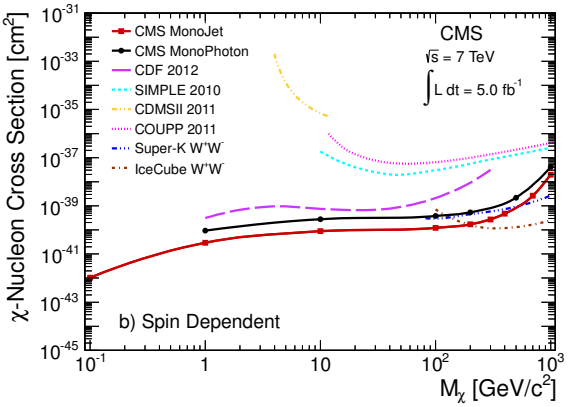

Figure 2. Comparison of the 90% CL upper limits on the dark matter-nucleon scattering cross section versus dark matter mass for the spin-dependent (axial-vector coupling) models with results from various direct detection experiments

5. Conclusion

We performed a search for new physics using 5 fb^{-1} of $\sqrt{7}$ TeV collisions in CMS for a signal of $\not{E}_T$ along with either a photon or a jet. In both cases, observation agrees with the SM, so limits were computed for the DM particle mass and it's nucleon scattering cross section in the

Table 3. Monophoton observed (expected) 90% C.L. limits on DM model parameters.

M_χ[GeV]	Vector		Axial-Vector	
	σ [fb]	Λ [GeV]	σ [fb]	Λ [GeV]
1	14.3 (14.7)	572 (568)	14.9 (15.4)	565 (561)
10	14.3 (14.7)	571 (567)	14.1 (14.5)	573 (569)
100	15.4 (15.3)	558 (558)	13.9 (14.3)	554 (550)
200	14.3 (14.7)	549 (545)	14.0 (14.5)	508 (504)
500	13.6 (14.0)	442 (439)	13.7 (14.1)	358 (356)
1000	14.1 (14.5)	246 (244)	13.9 (14.3)	172 (171)

Table 4. Monojet observed 90% C.L. limits on DM model parameters.

M_χ[GeV]	Vector		Axial-Vector	
	σ $[cm^2]$	Λ [GeV]	σ $[cm^2]$	Λ [GeV]
0.1	749	$2.90 \cdot 10^{-41}$	754	$1.03 \cdot 10^{-42}$
1	751	$8.21 \cdot 10^{-40}$	755	$2.94 \cdot 10^{-41}$
10	760	$2.47 \cdot 10^{-39}$	765	$8.79 \cdot 10^{-41}$
100	764	$2.83 \cdot 10^{-39}$	736	$1.21 \cdot 10^{-40}$
200	736	$3.31 \cdot 10^{-39}$	677	$1.70 \cdot 10^{-40}$
300	690	$4.30 \cdot 10^{-39}$	602	$2.73 \cdot 10^{-40}$
400	631	$6.15 \cdot 10^{-39}$	524	$4.74 \cdot 10^{-40}$
700	455	$2.28 \cdot 10^{-38}$	341	$2.65 \cdot 10^{-39}$
1000	302	$1.18 \cdot 10^{-37}$	206	$1.98 \cdot 10^{-38}$

regime of a high cut off scale. For spin-independent DM models, this analysis extends the limits on the DM-nucleon scattering cross section for DM particles below about 3.5 GeV, which was inaccessible to direct detection experiments. For spin-dependent models, this analysis provides the most stringent limits on the DM-nucleon scattering cross section for DM particles within the DM mass range of 1-1000 GeV.

References

[1] Gaitskell R 2004 *Annual Review of Nuclear and Particle Science* **54**
[2] CMS Collaboration (CMS) 2008 *Journal of Instrumentation* **3** S08004 URL http://stacks.iop.org/1748-0221/3/i=08/a=S08004
[3] Bai Y, Fox P J and Harnik R 2010 *JHEP* **12** 048 (*Preprint* 1005.3797v2)
[4] Fox P J, Harnik R, Kopp J and Tsai Y 2011 Missing energy signatures of dark matter at the lhc Tech. rep. Fermilab (*Preprint* 1109.4398)
[5] CMS Collaboration (CMS) 2009 Particle–flow event reconstruction in CMS and performance for jets, taus, and $\not{E}_T$ CMS Physics Analysis Summary CMS-PAS-PFT-09-001 CERN URL http://cdsweb.cern.ch/record/1194487
[6] Cacciari M, Salam G P and Soyez G 2008 *JHEP* **04** 063 (*Preprint* 0802.1189)
[7] CMS Collaboration (CMS) 2010 Electromagnetic calorimeter commissioning and first results with 7 tev data CMS Physics Analysis Summary CMS-NOTE-2010-012 CERN URL http://cdsweb.cern.ch/record/1278160
[8] Aaltonen T *et al.* (CDF) 2012 *Phys. Rev. Lett.* **108**(21) 211804 (*Preprint* 1203.0742)
[9] Behnke E *et al.* (COUPP) 2011 *Phys. Rev. Lett.* **106**(2) 021303 (*Preprint* 1008.3518) URL http://link.aps.org/doi/10.1103/PhysRevLett.106.021303
[10] Aalseth C E *et al.* (CoGeNT) 2011 *Phys. Rev. Lett.* **106**(13) 131301 (*Preprint* 1002.4703) URL http://link.aps.org/doi/10.1103/PhysRevLett.106.131301
[11] Archambault S *et al.* 2009 *Phys. Lett. B* **682** 185 ISSN 0370-2693 (*Preprint* 0907.0307) URL http://www.sciencedirect.com/science/article/pii/S0370269309013525
[12] Aprile E *et al.* (XENON100) 2011 *Phys. Rev. Lett.* **107**(13) 131302 (*Preprint* 1104.2549) URL http://link.aps.org/doi/10.1103/PhysRevLett.107.131302
[13] CDMS II Collaboration (CDMS II) 2010 *Science* **327** 1619 (*Preprint* http://www.sciencemag.org/content/327/5973/1619.full.pdf)
[14] Ahmed Z *et al.* (CDMS) 2011 *Phys. Rev. Lett.* **106**(13) 131302 (*Preprint* 1011.2482) URL http://link.aps.org/doi/10.1103/PhysRevLett.106.131302
[15] Felizardo M, Morlat T, Fernandes A C, Girard T A, Marques J G, Ramos A R, Auguste M, Boyer D, Cavaillou A, Sudre C, Poupeney J, Payne R F, Miley H S and Puibasset J (SIMPLE) 2010 *Phys. Rev. Lett.* **105** 211301 a more recent update can be found in http://arxiv.org/abs/1106.3014 arXiv:1106.3014 (*Preprint* 1003.2987)
[16] Abbasi R *et al.* (IceCube) 2012 *Phys. Rev. D* **85** 042002 (*Preprint* 1112.1840)
[17] Tanaka T *et al.* (Super-Kamiokande) 2011 *Astrophys. J.* **742** 78 (*Preprint* 1108.3384)